



Published in final edited form as:

*Mov Disord.* 2020 May ; 35(5): 760–773. doi:10.1002/mds.27994.

## Lysosome and Inflammatory Defects in *GBA1*-Mutant Astrocytes Are Normalized by LRRK2 Inhibition

Anwasha Sanyal, PhD<sup>#1</sup>, Mark P. DeAndrade, PhD<sup>#1</sup>, Hailey S. Novis, BS<sup>1</sup>, Steven Lin, BS<sup>1</sup>, Jianjun Chang, MS<sup>2</sup>, Nathalie Lengacher, BS<sup>3</sup>, Julianna J. Tomlinson, PhD<sup>3</sup>, Malú G. Tansey, PhD<sup>4</sup>, Matthew J. LaVoie, PhD<sup>1,\*</sup>

<sup>1</sup>Ann Romney Center for Neurological Diseases, Brigham and Women's Hospital and Harvard Medical School, Boston, Massachusetts, USA

<sup>2</sup>Department of Physiology, Emory University School of Medicine, Atlanta, Georgia, USA

<sup>3</sup>Program in Neuroscience, Ottawa Hospital Research Institute, University of Ottawa Brain and Mind Research Institute, Ottawa, Ontario, Canada

<sup>4</sup>Department of Neuroscience and Center for Translational Research in Neurodegenerative Disease, Norman Fixel Institute for Neurological Diseases, University of Florida College of Medicine, Gainesville, Florida, USA

# These authors contributed equally to this work.

### Abstract

**Background**—Autosomal recessive mutations in the glucocerebrosidase gene, *Beta-glucocerebrosidase 1 (GBA1)*, cause the lysosomal storage disorder Gaucher's disease. Heterozygous carriers of most *GBA1* mutations have dramatically increased Parkinson's disease (PD) risk, but the mechanisms and cells affected remain unknown. Glucocerebrosidase expression is relatively enriched in astrocytes, yet the impact of its mutation in these cells has not yet been addressed.

**Objectives**—Emerging data supporting non-cell-autonomous mechanisms driving PD pathogenesis inspired the first characterization of *GBA1*-mutant astrocytes. In addition, we asked whether LRRK2, likewise linked to PD and enriched in astrocytes, intersected with *GBA1* phenotypes.

**Methods**—Using heterozygous and homozygous *GBA1 D409V* knockin mouse astrocytes, we conducted rigorous biochemical and image-based analyses of lysosomal function and morphology. We also examined basal and evoked cytokine response at the transcriptional and secretory levels.

**Results**—The *D409V* knockin astrocytes manifested broad deficits in lysosomal morphology and function, as expected. This, however, is the first study to show dramatic defects in basal and TLR4-dependent cytokine production. Albeit to different extents, both the lysosomal dysfunction

\*Correspondence to: Dr. M.J. LaVoie, Hale Building for Transformative Medicine, Room 10016M, 60 Fenwood Road, Boston, MA 02115, mlavoie@rics.bwh.harvard.edu.

Relevant conflicts of interests/financial disclosures: Nothing to report.

and inflammatory responses were normalized by inhibition of LRRK2 kinase activity, suggesting functional intracellular crosstalk between glucocerebrosidase and LRRK2 activities in astrocytes.

**Conclusions**—These data demonstrate novel pathologic effects of a *GBA1* mutation on inflammatory responses in astrocytes, indicating the likelihood of broader immunologic changes in GBA-PD patients. Our findings support the involvement of non-cell-autonomous mechanisms contributing to the pathogenesis of *GBA1*-linked PD and identify new opportunities to correct these changes with pharmacological intervention.

### Keywords

astrocyte dysfunction; GBA1; LRRK2; neuroinflammation; Parkinson's disease

---

Growing genetic and biochemical evidence place lysosomal dysfunction at the center of pathogenic mechanisms underlying Parkinson's disease (PD).<sup>1–6</sup> The vast majority of preclinical studies have focused on how PD mutations affect lysosome function in neurons.<sup>7–12</sup> Importantly, the impact of these mutations in non-neuronal cells has been virtually ignored despite clear evidence of reactive gliosis in the human disease and preclinical models of nigrostriatal degeneration<sup>13–22</sup> and the enriched expression of these gene products in glial cells.<sup>23,24</sup> To address this unmet need, we focused on the effects of a lysosomal protein associated with PD risk and enriched in astrocytes, which constitute at least one-third of the brain.<sup>23,25</sup>

Glucocerebrosidase (GCase), encoded by *GBA1* gene, is a lysosomal enzyme that catalyzes the conversion of the glycolipid glucosylceramide into glucose and ceramide. Autosomal recessive loss-of-function mutations in *GBA1* cause the lysosomal storage disorder Gaucher's disease, which frequently presents with severe neurologic complications.<sup>26–28</sup> However, heterozygous carriers of specific mutations in *GBA1* are subject to dramatically elevated risk of PD.<sup>29,30</sup> GBA-PD shares many of the classic clinical features of idiopathic PD, including levodopa-responsive motor symptoms, age-dependent accumulation of  $\alpha$ -synuclein, and the formation of Lewy bodies.<sup>31–33</sup> The pathways through which *GBA1* mutations affect PD risk are entirely unknown. Interestingly, GCase mRNA and protein is highly enriched within human and murine astrocytes,<sup>23</sup> yet the impact of *GBA1* mutations on astrocyte function and inflammatory responses has not yet been considered.

Here we explored primary cultured astrocytes from mice harboring the heterozygous or homozygous knockin *GBA1 D409V* mutation associated with PD and compared these cells to those expressing wild-type (WT) *GBA1*. Our data showed the expected gene-dose effect on GCase activity as well as a complex series of defects in lysosomal function. We then asked whether these effects translated into deficits in the degradation of exogenously applied monomeric or fibrillar  $\alpha$ -synuclein. Although *GBA1* mutation results in intrinsic decreases in lysosomal protease activity, it had no effect on astrocyte-mediated degradation of  $\alpha$ -synuclein. We then investigated a central feature of astrocyte biology, that is, whether *GBA1* mutation altered cytokine production. Although some cytokines were unaffected, the results showed a dramatic decrease in the expression and secretion of several proinflammatory cytokines from *GBA1*-mutant astrocytes. Given the established role of leucine-rich repeat kinase 2 (LRRK2) in both lysosome function and inflammatory responses,<sup>6,9,34–39</sup> the

primary outcomes affected by the *GBA1* mutation in this study, we examined how LRRK2 kinase inhibition would influence the mutant *GBA1* phenotypes. The results showed that LRRK2 inhibition normalized a subset of the lysosomal abnormalities, with a near restoration of cytokine production by *GBA1*-mutant astrocytes. Notably, this normalization was more profound in the heterozygous (PD model) of astrocytes than that observed in the homozygous mutant (Gaucher's model) cells. These are perhaps the first data to demonstrate crosstalk between the GCase protein and LRRK2 kinase activity, but may not be surprising given the role of LRRK2 in regulating intracellular trafficking<sup>40–42</sup> and that proper folding and lysosomal localization of GCase is essential to its normal function.<sup>43,44</sup> The LRRK2–GCase interaction identified here may advance our understanding of familial and sporadic PD, but more specifically provide insight into emerging analyses of patients carrying both *GBA1* and *LRRK2* mutations and their complex presentation.<sup>45</sup>

These data are the first to demonstrate a pathogenic role of *GBA1* mutations in astrocyte dysfunction and that *GBA1*-induced inflammatory responses may contribute to neurologic damage and an increased risk for PD. Our observation of novel immune responses unique to the heterozygous *GBA1* mutation, and the notable expression of GCase in a host of peripheral immune cells, suggest that GBA-PD patients should be investigated through the prism of peripheral immunologic responses, as is currently underway with respect to LRRK2-PD. GBA-PD patients may manifest immunologic profiles congruent with sporadic PD or entirely novel characteristics. The power of the longitudinal assessment of this large *GBA1* carrier cohort may allow for peripheral immune profiles to ultimately track disease progression or distinguish *GBA1* carriers destined to develop PD features from those who are not.

## Materials and Methods

### Primary Astrocyte Culture

Mouse primary astrocytes were isolated as previously described<sup>46</sup> with certain modifications. On day 3, the media was changed. On day 7, the astrocytes were shaken at 180 rpm for 30 minutes followed by 240 rpm for 60 minutes at 37°C. On day 8, the cells were plated for experiments.

### Western Blot

Cells lysates were prepared as previously described.<sup>6</sup> Nuclear fractionation was conducted as previously described.<sup>47</sup> For dot blots, total protein was blotted on a nitrocellulose membrane without boiling. The blots were probed with primary antibodies to Lysosomal Associated Membrane Protein 1 (Abcam (Cambridge, MA) ab108597), GCase (Abcam ab55080), cathepsin D (Abcam ab6313), Transcription Factor EB (Abcam ab220695), phospho LRRK2 (Abcam 133450), LRRK2 (clone D8629),  $\alpha$ -synuclein preformed fibrils (PFF; Abcam ab209538).

### Immunofluorescence

Cells were washed with phosphate-buffered saline (PBS), fixed with 4% (w/v) paraformaldehyde, blocked with 5% (v/v) bovine serum albumin in PBS for 30 minutes, and

permeabilized with 0.1% (v/v) Triton X-100 in PBS for 5 minutes. A primary antibody to glial fibrillary protein (GFAP; Abcam ab7260), NeuN (Sigma MAB377 (St. Louis, MO)) and CD11b (Novex (Bedford, MA) NB110–89474) was incubated for 1 hour and washed with PBS; the secondary antibody conjugated to Alexa Fluor dye was incubated for 1 hour, washed with PBS, and visualized by confocal microscopy (Zeiss (Jena, Germany) LSM710).

### Flow Cytometry

About  $1 \times 10^6$  cells were harvested in 1 mL of PBS and centrifuged for 5 minutes at 500g. The pellet was resuspended in 0.1% Triton-X, incubated for 10 minutes, and centrifuged for 5 minutes at 500g. The supernatant was removed and the cells were resuspended in 5% bovine serum albumin for 30 minutes. The cells were then centrifuged for 5 minutes at 500g and resuspended in primary antibody (GFAP Abcam ab7260, Cd11B BioRad (Portland, ME) MCA711G) at a dilution of 1:100 and incubated for 1 hour at room temperature. The cells were centrifuged for 5 minutes at 500g and resuspended in the secondary antibody (Alexa Fluor 488 A10680, Alexa Fluor 564 A21442; Invitrogen (Bedford, MA)) at a dilution of 1:500 and incubated for 1 hour at room temperature in the dark. Cells were centrifuged for 5 minutes at 500g, and the pellet was resuspended in 1 mL of PBS. BD LSR II was used to sort the cells, and FlowJo LLC, Ashland, OR software was used to analyze the samples.

### GCCase Activity Assay

Assay was conducted as previously described.<sup>48</sup>

### High-Content Analysis of Lysosomal Morphology

A total of 10,000 astrocytes were plated per well in 96-well black wall clear bottom plates (Greiner, Bedford, MA) and labeled with LysoTracker Red (Invitrogen) according to the manufacturer's specifications and 20 ng/mL of Hoechst. Labeled live cells were imaged as previously described.<sup>6</sup>

### LysoSensor Assay

For lysosomal pH analysis, the ratiometric dye LysoSensor Yellow/Blue (Invitrogen) was used to label 10,000 astrocytes per well in 96-well black wall black bottom plates (Greiner) as previously described.<sup>6</sup>

### DQ-BSA Assay

For lysosomal protease activity analysis, 10,000 astrocytes were plated per well in 96-well plates (Greiner) and labeled with DQ-BSA dye (1  $\mu$ M) for 10 minutes and 20 ng/mL of Hoechst prior to rinsing 2 times with HBSS buffer. The cells were imaged using a Synergy H1 hybrid reader (Biotek; excitation 329/384 nm, emission 440/540 nm).

### Cathepsin Activity Assays

A total of 10,000 astrocytes were plated per well in 96-well plates (Greiner) and labeled with 1  $\mu$ M Magic-Red dye (Bio-Rad) for 10 minutes and 20 ng/mL of Hoechst prior to rinsing 2 times with HBSS buffer. The cells were imaged using a Synergy H1 hybrid reader (Biotek;

excitation 329/384 nm, emission 440/540 nm). Cathepsin D activity assay was conducted as per the manufacturer's protocol (Abcam ab65302).

### Multiplexed Immunoassays

Levels of immune factors were measured using the V-PLEX Proinflammation Panel 1 Kit (mouse; Meso Scale Discovery, Rockville, MD) according to the manufacturer's protocol by the Emory Multiplexed Immunoassay Core. Conditioned media were run in duplicate and were diluted by a factor of 1 or 2. Analyte levels were measured on the Meso Scale Discovery QuickPlex instrument and evaluated on the Meso Scale Discovery software platform.

### RNA Isolation, RT, and qRT-Polymerase Chain Reaction

Total cell RNA was extracted with the RNeasy Mini Plus Kit (Qiagen, Germantown, MD), and 5  $\mu$ g of RNA was reverse transcribed with random primers using the Superscript IV First Strand Synthesis System (Life Technologies, Bedford, MA). A total of 2  $\mu$ L of a 1:10 dilution of cDNA was used for quantitative polymerase chain reaction with gene specific primers and SYBR Green PCR Master Mix (Applied Biosystems, Bedford, MA) according to the manufacturer's instructions. Mouse gene-specific primer sequences are the following: IL1 $\beta$  (forward 5'-CAGGCAGGCAGTATCACTCA-3', reverse 5'-TGTCCTCATCCTGGAAGGTC-3;), Tumor necrosis factor (forward 5'-ACGGCATGGATCTCAAAGAC-3', reverse 5'-GTGGGTGAGGAGCACGTAGT-3'), IL6 (forward 5'-ATGGATGCTACCAAAGTGGAT-3', reverse 5'-TGAAGGACTCTGGCTTTGTCT-3'), Interleukin 12 (forward 5'-AAGCTCTGCATCCTGCTTAC-3', reverse 5'-GATAGCCCATCACCTGTTGA-3'), Lipocalin-2 (forward 5'-TTTCACCCGCTTTGCAAGT-3', reverse 5'-GTCTCTGCGCATCCAGTCA-3'), CXCL1 (forward 5'-TGAGCTGCGCTGTCAGTGCCT-3', reverse 5'-AGAAGCCAGCGTTCACCAGA-3'), Inducible nitric oxide synthase (forward 5'-GGCAGCCTGTGAGACCTTTG-3', reverse 5'-GCATTGGAAGTGAAGCGTTTC-3'), Glyceraldehyde 3-phosphate dehydrogenase (forward 5'-AACTTTGGCATTGTGGAAGGGCTC-3', reverse 5'-GGAAGAGTGGGAGTTGCTGTTGA-3'), ACTIN (forward 5'-GAAATCGTGCGTGACATCAAAG-3', reverse 5'-TGTAGTTTCATGGATGCCACAG-3').

### Statistical Analyses

All experiments were conducted at least 3 independent times. Error bars indicate mean  $\pm$  standard error of mean. Statistical analysis was performed using GraphPad (San Diego, CA) Prism software using a 1-way or 2-way analysis of variance with Tukey's post hoc test.

## Results

### **GBA1 D409V Knockin Mutation Causes Lysosomal Impairment in Mouse Primary Astrocytes**

Mutations at the D409 locus in the GBA1 protein are associated with both PD risk and Gaucher's disease.<sup>49,50</sup> Interestingly, GCase is one of a handful of PD-linked proteins

relatively enriched in astrocytes, the most abundant cell type in the brain. Therefore, we cultured primary mouse astrocytes from *GBA1 D409V* heterozygous and homozygous knockin mice to consider the non-cell-autonomous effect of a *GBA1* mutation. We tested the purity of the primary astrocyte cultures by flow cytometry following immunofluorescence staining for astrocytes (GFAP), microglia (CD11b), and neurons (NeuN). The cultures were relatively pure (~98% by GFAP) with limited contamination (~2%) likely comprising of microglia and/or oligodendrocytes (Fig. 1A). Next, we examined the immunologic responsiveness of these cultures. Induction of maximal response with LPS for 6 and 24 hours manifested a classic TLR4-dependent inflammatory response as indicated by the upregulation of IL6, IL1 $\beta$ , TNF, and iNOS mRNA (Fig. 1B). We confirmed the predicted impact of a *GBA1* mutation on GCCase activity levels in this cell type using a GCCase-specific fluorogenic substrate. We found GCCase activity was reduced to 47% of control in heterozygous *D409V* and 8% in homozygous *D409V* knockin astrocytes (Fig. 1C), demonstrating the classic gene-dose response reported in other cells.<sup>51</sup> Prior studies have suggested that a *GBA1* mutation evokes broad effects on lysosome behavior.<sup>52-55</sup> Hence, we sought to determine the effects of endogenous *GBA1 D409V* mutation on lysosome function in astrocytes. We quantified the number of lysosomes per cell by high-content image analysis. The results indicated a significant reduction (51%) in lysosome count per cell in the heterozygous mutant with a greater reduction (69%) in the homozygous mutant astrocytes (Fig. 1D), consistent with the gene-dose relationship observed for GCCase activity (Fig. 1C). However, the average area of individual lysosomes remained unchanged (Fig. 1E). This quantification of lysosome count was determined by LysoTracker staining, but the efficiency of labeling can be influenced by lysosome pH. To control for this, independent experiments used LAMP2 staining yielded similar data (data not shown). Interestingly, LAMP1 and nuclear TFEB remain unchanged in their expression levels, suggesting no obvious deficit in lysosome biogenesis (Fig. 1F). Furthermore, GCCase protein levels were unchanged (Fig. 1F) despite substantial changes in GCCase activity (Fig. 1C). We did observe reduced colocalization of LAMP1 and LAMP2, further indicating lysosomal impairment (Fig. 1G). Next, we analyzed the luminal pH of these lysosomes using a ratiometric pH-sensitive dye, LysoSensor. Lysosomes in the heterozygous and homozygous *GBA1*-mutant astrocytes were both significantly alkalinized to a similar degree (pH~6) when compared with the WT control (Fig. 2A). Lysosomes require an acidic pH for optimal functioning. Thus, we hypothesized that the *GBA1*-mutant lysosomes would perturb lysosome protease function. We examined general protease activity in these lysosomes using an autoquenched DQ-BSA conjugate dye. Upon exposure to active proteases, the conjugate is cleaved into unquenched fluorescent peptide fragments. Using this assay, we found that the general lysosome protease activity was unchanged in the heterozygous mutant but was significantly decreased in the homozygous mutant lysosomes (Fig. 2B). We then analyzed the activity of individual lysosomal proteases. Data showed that although cathepsin D (Fig. 2C) and L (Fig. 2D) activity remain unaffected, cathepsin B activity was decreased in both heterozygous and homozygous mutant lysosomes (Fig. 2E). These data together indicate a subtle loss of lysosomal protease activity induced by a *GBA1* mutation, likely as a result of luminal alkalinization.

### LRRK2 Kinase Inhibition Rescues Decreased *GBA1*-Induced Lysosomal Function

We previously reported that LRRK2 inhibition has a mild acidifying effect on WT lysosomes and an enhanced effect on aberrantly alkalinized lysosomes.<sup>6</sup> Therefore, we asked whether LRRK2 kinase inhibition could reacidify lysosomes in *GBA1*-mutant astrocytes. To date, MLi-2 has been found to be the most potent and selective LRRK2 kinase inhibitor. The IC<sub>50</sub> of MLi-2 for LRRK2 is in the low nanomolar range and offers better pharmacokinetics than other commonly used LRRK2 inhibitors.<sup>56</sup> Thus, we treated WT and *GBA1*-mutant astrocytes with MLi-2 and found that LRRK2 kinase inhibition decreased the alkaline lysosomal pH in *GBA1* mutants (Fig. 3A). Two-way analyses of variance revealed a significant genotype–treatment interaction effect, as pH was not altered by treatment in WT cells, but was significantly reduced in homozygous mutant astrocytes and trended toward decreased pH in the heterozygous mutant cells. In addition, the lysosomal pH of all LRRK2 inhibitor-treated cells was no longer significantly different from untreated WT cells, suggesting normalization of lysosomal pH. However, the deficits in lysosomal number were not reversed (Fig. 3B), and the average lysosomal area remain unaffected by this treatment (Fig. 3C). Lastly, we found that the reduced cathepsin B activity in the heterozygous *GBA1* cells was significantly rescued by 7-day treatment with MLi-2. Interestingly, LRRK2 kinase inhibition could not rescue the more severe cathepsin B deficit in homozygous mutant astrocytes (Fig. 3D). Together, these data indicate that LRRK2 kinase inhibition has a partial and selective effect on reversing some *GBA*-induced deficits.

### *GBA1 D490V* Mutation Induces Downregulation in Endogenous WT LRRK2 Kinase Activity

Because *GBA1*-induced lysosomal dysfunction was rescued by LRRK2 kinase inhibition, we speculated that *GBA1* mutants had intrinsically increased LRRK2 kinase activity and that rescue was attributable to correcting this increase. We first examined the phosphorylation status of LRRK2 S935, an indirect marker of LRRK2 activity,<sup>57</sup> and observed a subtle decrease in *GBA1*-mutant astrocytes (Fig. S1A). Phosphorylation of LRRK2 S1292, a putative autophosphorylation site, was not detectable using commercially available antibody (not shown). We then sought greater resolution and analyzed the phosphorylation levels of recently discovered LRRK2 substrates, Rab10 and Rab8a.<sup>41</sup> Here too we found the phosphorylation status of both Rab10 (Fig. S1B) and Rab8a (Fig. S1C) significantly decreased in the heterozygous and homozygous mutant astrocytes, confirming a decrease in LRRK2 kinase activity. Critically, the total protein levels of Rab10, Rab8a, and LRRK2 were unchanged across all genotypes and treatments.

### *GBA1 D490V* Mutation Exerts No Effect on $\alpha$ -Synuclein Degradation by Astrocytes

Astrocytes are known to phagocytize and degrade extracellular  $\alpha$ -synuclein in both *in vitro* and *in vivo* brain slice models,<sup>58,59</sup> which depends partly on a fully functional endo-lysosomal system. Thus, we hypothesized that *GBA1*-mutant astrocytes may be deficient with respect to the degradation of extracellular  $\alpha$ -synuclein. We exposed WT and mutant astrocytes to monomeric or PFF of  $\alpha$ -synuclein and allowed for uptake and monitored degradation over time (1–16 hours; Fig. S2A). The levels of remaining intracellular monomeric  $\alpha$ -synuclein, as quantified by enzyme-linked immunosorbent assay, were indistinguishable between genotypes (Fig. S2B). In separate experiments, the cellular levels

of  $\alpha$ -synuclein PFFs were determined by detection with  $\alpha$ -synuclein filament-specific structural antibody (MJFR 14–6–4–2). Similar to a monomer, PFFs were degraded at similar rates by WT and *GBA1*-mutant astrocytes (Fig. S2C). These data suggest that the subtle lysosomal deficits in *GBA1*-mutant astrocytes are insufficient to affect their ability to degrade  $\alpha$ -synuclein; perhaps *GBA1* mutations in astrocytes contribute to pathogenesis via other mechanisms.

### ***GBA1* D490V Mutation Effects Selective Inflammatory Response in Astrocytes That Can Be Rescued by LRRK2 Kinase Inhibition**

Here we asked whether *GBA1*-mutant astrocytes were affected in their response to inflammatory stimuli. To our surprise, quantitative polymerase chain reaction analysis of mRNA levels revealed that the basal levels of proinflammatory cytokine (IL6, IL1 $\beta$ , TNF, and IL12p70) and chemokine (CXCL1, iNOS, and LCN2) expression was significantly decreased in naïve *GBA* mutant astrocytes when compared with controls (Fig. 4A). Of note, some anti-inflammatory cytokines were either not in the detectable range (IL4 and IL10) or were unchanged (IL2, IL5, and IFN $\gamma$ ; not shown). Next, we treated cells with the TLR4 agonist LPS to analyze maximal cytokine response. Consistently, LPS-evoked cytokine/chemokine expression was likewise dramatically reduced by *GBA1* mutation (Fig. 4B). We had observed that the LRRK2 kinase inhibitor MLI-2 rescued the alkalinized lysosome phenotype in *GBA1*-mutant astrocytes. Hence, we asked whether this rescue extended to other functional deficits caused by *GBA1* mutation. We observed that the mRNA levels of proinflammatory cytokines and chemokines were normalized to WT levels by LRRK2 kinase inhibition in *GBA1* heterozygous cells (Fig. 5A). Interestingly, some cytokines in homozygous mutant astrocytes were not normalized. A functional readout for inflammatory responsiveness is the secretion of cytokines. Thus, we quantified the levels of cytokines in the conditioned media from the naïve astrocytes using a multiplex immunoassay and found significantly decreased secretion in mutant astrocytes when compared with WT. Similar to rescue of cytokine expression (mRNA), MLI-2 normalized cytokine secretion in *GBA1* heterozygous cells (Fig. 5B). These data indicate a robust deficit in upstream transcriptional regulatory mechanisms governing inflammatory responsiveness in *GBA1*-mutant astrocytes, which may contribute significantly to immune dysfunction and increased *GBA1*-linked PD risk.

## **Discussion**

Near-complete loss of GCase activity causes the lysosomal storage disorder, Gaucher's disease, where ~300 different mutations in *GBA1* drive disease through autosomal recessive inheritance.<sup>28</sup> Increasing evidence, however, associates partial GCase loss of function with parkinsonism as heterozygous carriers of *GBA1* mutations are at a significantly higher risk of PD.<sup>60–63</sup> Genetic studies show that 5% to 10% of people with PD harbor a *GBA1* mutation.<sup>64–67</sup> Perhaps not surprising then, a significantly higher number of Gaucher's disease patients have comorbidity with parkinsonism.<sup>68</sup> Despite such a strong correlation between *GBA1* and PD, the mechanisms underlying this increased risk remain elusive. Moreover, the specific cell types in which these mutations are expressed to influence disease course is likewise unknown. Growing evidence across many age-related neurodegenerative



diseases endorses a primary and active role of glial dysfunction in the demise of neurons, not simply a consequence of neurologic disease.<sup>69-74</sup> Therefore, non-neuronal cells must be considered in the pathogenesis and progression of disease caused by PD-linked mutations.

Astrocytes are emerging as critical players in the pathogenesis of many neurologic and psychiatric diseases.<sup>75-80</sup> To explore non-cell-autonomous mechanisms of the *GBA1* mutation, we analyzed primary cultured astrocytes from WT and heterozygous and homozygous *D409V GBA1* knockin mice and observed broad lysosomal impairment in *GBA1*-mutant astrocytes. Similar deficits in lysosomal proteases have also been observed in *GBA1*-mutant neurons and patient fibroblasts.<sup>1,81</sup> Interestingly, our data also showed that *GBA1*-mutant astrocytes possessed a severe deficit in inflammatory responsiveness in both naïve and LPS-stimulated cytokine production. This was observed both at the mRNA and protein levels, suggesting that these effects are far upstream at the transcriptional level. These are the first data demonstrating immunologic changes in *GBA1*-mutant glia.

Neurons can release  $\alpha$ -synuclein,<sup>82,83</sup> and the accumulation of  $\alpha$ -synuclein within astrocytes has been reported in the PD brain.<sup>84,85</sup> Therefore, glia are likely exposed to extracellular  $\alpha$ -synuclein and possess the opportunity to mitigate the transmission of the neuronally released  $\alpha$ -synuclein.<sup>86,87</sup> Thus, we hypothesized that *GBA1*-mutant astrocytes may be ineffective in clearing extracellular  $\alpha$ -synuclein. However, data revealed that mutant *GBA1* astrocytes degrade both exogenously applied  $\alpha$ -synuclein monomer and PFF at the same rate as WT astrocytes, suggesting that the lysosomal abnormalities associated with the *GBA1* mutation do not directly affect the specific processes involved in the degradation of extracellular  $\alpha$ -synuclein.

Similar to *GBA1*, autosomal-dominant mutations in the *LRRK2* gene cause familial PD. *LRRK2* is likewise known to exert lysotropic effects, and both *LRRK2* and GCCase expression is enriched in astrocytes.<sup>23,88</sup> Recent work from our group demonstrated that *LRRK2* kinase inhibitors increase lysosomal acidification, with greater effects observed when lysosomes were aberrantly alkalinized,<sup>6</sup> as was the case with the *GBA1* mutation (Fig. 2C). We therefore hypothesized that inhibition of *LRRK2* may normalize a subset of lysosomal defects observed in the *GBA1*-mutant astrocytes. The results showed a reacidification of lysosomal pH and a correction of cathepsin B activity following *LRRK2* inhibitor treatment. We then probed further to determine how *LRRK2* kinase inhibition would impact the *GBA1*-induced suppression of cytokine release. We found that *LRRK2* inhibition corrected the *GBA1*-induced suppression of cytokine expression (mRNA) and secretion (protein) for both basal and LPS-stimulated responses. Collectively, these data demonstrate a previously unrecognized crosstalk between broad cellular phenotypes caused by the *GBA1* mutation and the physiologic function of *LRRK2*. These data are also consistent with a very recent finding that *LRRK2* kinase inhibition can increase GCCase activity in WT cells and even in cells where it is reduced by *GBA* or *LRRK2* mutation.<sup>89</sup>

Given the normalizing effects of *LRRK2* inhibition, we speculated that the intrinsic activity of *LRRK2* was increased in *GBA1*-mutant cells and that the effects we observed were through a corrective *LRRK2* reduction to baseline. Surprisingly, multiple markers of *LRRK2* activity were decreased in the *GBA1*-mutant astrocytes, further underscoring the crosstalk

between mutant GCase activity and LRRK2. We hypothesize that the *GBA1*-mutant astrocytes initiated an endogenous downregulation of LRRK2 kinase activity as a compensatory effort by the cells to attenuate the pathogenic effects of *GBA1* mutation. However, this intrinsic effect is not sufficient to fully rescue the defects in lysosome function and response to inflammatory signals, as further inhibition via pharmacologic means normalized *GBA1*-induced phenotypes in the heterozygous state. It is likely that evidence of this novel *GBA1*–LRRK2 crosstalk has also been observed in the clinic. It would be expected that patients carrying pathogenic mutations in both *GBA1* and *LRRK2* would manifest additive features of each individual mutation, if not potentiated deficits. However, in a small clinical study it was observed that patients with both a *GBA1* mutation and the G2019S *LRRK2* mutation had decreased risk for many of the *GBA1*-associated complications, as if the LRRK2 mutation had mitigated some of the effects of mutant *GBA1*.<sup>45</sup> These data, along with our findings, demonstrate a pressing need to understand the intersection of GCase and LRRK2 biology at both the cellular level and in patients carrying these mutations.

Reactive gliosis and neuroinflammation are well-documented features of PD. Although early studies focused on phagocytic microglia within the substantia nigra pars compacta,<sup>17,90,91</sup> an important involvement of astrocytes has since been established.<sup>72,92–94</sup> Here, we demonstrate for the first time a critical effect of *GBA1* mutation on the immunologic responsiveness of astrocytes. Although pathologic *GBA1*-induced changes in cytokines may have been expected to increase their release, our data would be consistent with emerging studies of decreased cytokine responsiveness observed in aging models,<sup>95</sup> acknowledging aging as the greatest risk factor for sporadic PD. Familial and sporadic PD share a number of overlapping clinical features, including  $\alpha$ -synuclein accumulation and motor symptoms. Our study indicates that immunologic changes may be another parallel between inherited and sporadic forms of the disease. Given the specific profile of cytokines and chemokines that were both affected and unaffected by the *GBA1* mutation and its high levels of expression in peripheral immune cells, our work may provide the impetus to investigate the *GBA1*-PD patient population for unique immunologic signatures in the peripheral blood of this cohort, as is currently underway for *LRRK2* mutation carriers. Perhaps immunologic responses may distinguish *GBA1* carriers predisposed to PD versus those who will not develop clinical features of PD. Such efforts may also identify overlapping or unique biomarkers for *GBA1*-PD, markers of disease progression, or further insights into familial and/or sporadic PD.

## Supplementary Material

Refer to Web version on PubMed Central for supplementary material.

## Acknowledgments

We thank Adam Canton for help with glucocerebrosidase activity assay. We are also grateful to Jason Schapansky, PhD, and other members of LaVoie lab for insightful discussions. This work was funded by the Michael J. Fox Foundation, American Parkinson Disease Association, and National Institutes of Health Grants NS065013 and NS069949 (M.J.L.) and a LRRK2 in Immunity LEAPS award (M.G.T.). This study was also supported in part by the Emory Multiplexed Immunoassay Core, which is subsidized by the Emory University School of Medicine and is one of the Emory Integrated Core Facilities. Additional support was provided by the National Center for Georgia Clinical & Translational Science Alliance of the National Institutes of Health under Award UL1TR002378. The

content is solely the responsibility of the authors and does not necessarily reflect the official views of the National Institutes of Health.

**Funding agencies:** Michael J. Fox Foundation, American Parkinson Disease Association, National Institutes of Health Grants NS110188 and NS069949 (M.J.L.) and NS092122 and a Michael J. Fox Foundation LRRK2 in immunity LEAPS award (M.G.T.).

## References

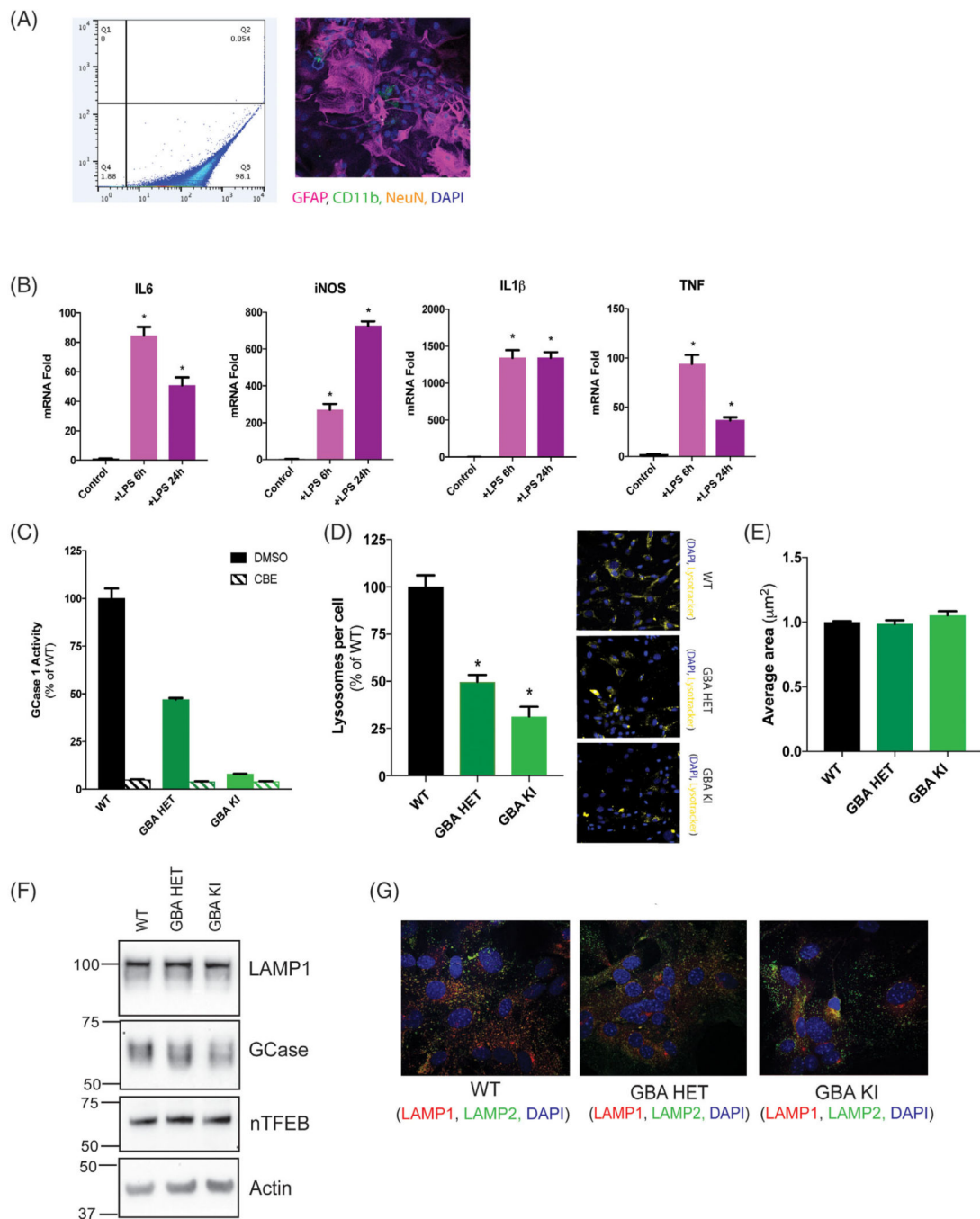
- Burbulla LF, Song P, Mazzulli JR, et al. Dopamine oxidation mediates mitochondrial and lysosomal dysfunction in Parkinson's disease. *Science* 2017;357(6357):1255–1261. [PubMed: 28882997]
- Chang D, Nalls MA, Hallgrimsdottir IB, et al. A meta-analysis of genome-wide association studies identifies 17 new Parkinson's disease risk loci. *Nat Genet* 2017;49(10):1511–1516. [PubMed: 28892059]
- Dehay B, Martinez-Vicente M, Ramirez A, et al. Lysosomal dysfunction in Parkinson disease: ATP13A2 gets into the groove. *Autophagy* 2012;8(9):1389–1391. [PubMed: 22885599]
- Lee HJ, Khoshaghideh F, Patel S, Lee SJ. Clearance of alpha-synuclein oligomeric intermediates via the lysosomal degradation pathway. *J Neurosci* 2004;24(8):1888–1896. [PubMed: 14985429]
- Mak SK, McCormack AL, Manning-Bog AB, Cuervo AM, Di Monte DA. Lysosomal degradation of alpha-synuclein in vivo. *J Biol Chem* 2010;285(18):13621–13629. [PubMed: 20200163]
- Schapansky J, Khasnavis S, DeAndrade MP, et al. Familial knockin mutation of LRRK2 causes lysosomal dysfunction and accumulation of endogenous insoluble alpha-synuclein in neurons. *Neurobiol Dis* 2018;111:26–35. [PubMed: 29246723]
- Dehay B, Ramirez A, Martinez-Vicente M, et al. Loss of P-type ATPase ATP13A2/PARK9 function induces general lysosomal deficiency and leads to Parkinson disease neurodegeneration. *Proc Natl Acad Sci U S A* 2012;109(24):9611–9616. [PubMed: 22647602]
- Henry AG, Aghamohammadzadeh S, Samaroo H, et al. Pathogenic LRRK2 mutations, through increased kinase activity, produce enlarged lysosomes with reduced degradative capacity and increase ATP13A2 expression. *Hum Mol Genet* 2015;24(21):6013–6028. [PubMed: 26251043]
- Hockey LN, Kilpatrick BS, Eden ER, et al. Dysregulation of lysosomal morphology by pathogenic LRRK2 is corrected by TPC2 inhibition. *J Cell Sci* 2015;128(2):232–238. [PubMed: 25416817]
- Jinn S, Drolet RE, Cramer PE, et al. TMEM175 deficiency impairs lysosomal and mitochondrial function and increases alpha-synuclein aggregation. *Proc Natl Acad Sci U S A* 2017;114(9):2389–2394. [PubMed: 28193887]
- Salerno DM, Gillingham KJ, Berry DA, Hodges M. A comparison of antiarrhythmic drugs for the suppression of ventricular ectopic depolarizations: a meta-analysis. *Am Heart J* 1990;120(2):340–353. [PubMed: 1696426]
- Sanchez-Danes A, Richaud-Patin Y, Carballo-Carbajal I, et al. Disease-specific phenotypes in dopamine neurons from human iPSC-based models of genetic and sporadic Parkinson's disease. *EMBO Mol Med* 2012;4(5):380–395. [PubMed: 22407749]
- Banati RB, Daniel SE, Blunt SB. Glial pathology but absence of apoptotic nigral neurons in long-standing Parkinson's disease. *Mov Disord* 1998;13(2):221–227. [PubMed: 9539333]
- Castano A, Herrera AJ, Cano J, Machado A. Lipopolysaccharide intranigral injection induces inflammatory reaction and damage in nigrostriatal dopaminergic system. *J Neurochem* 1998;70(4):1584–1592. [PubMed: 9580157]
- Gerhard A, Pavese N, Hotton G, et al. In vivo imaging of microglial activation with [11C](R)-PK11195 PET in idiopathic Parkinson's disease. *Neurobiol Dis* 2006;21(2):404–412. [PubMed: 16182554]
- Marinova-Mutafchieva L, Sadeghian M, Broom L, Davis JB, Medhurst AD, Dexter DT. Relationship between microglial activation and dopaminergic neuronal loss in the substantia nigra: a time course study in a 6-hydroxydopamine model of Parkinson's disease. *J Neurochem* 2009;110(3):966–975. [PubMed: 19549006]
- McGeer PL, Itagaki S, Boyes BE, McGeer EG. Reactive microglia are positive for HLA-DR in the substantia nigra of Parkinson's and Alzheimer's disease brains. *Neurology* 1988;38(8):1285–1291. [PubMed: 3399080]

18. Qiao C, Yin N, Gu HY, et al. Atp13a2 deficiency aggravates astrocyte-mediated neuroinflammation via NLRP3 inflammasome activation. *CNS Neurosci Ther* 2016;22(6):451–460. [PubMed: 26848562]
19. Barnum CJ, Chen X, Chung J, et al. Peripheral administration of the selective inhibitor of soluble tumor necrosis factor (TNF) XPro(R) 1595 attenuates nigral cell loss and glial activation in 6-OHDA hemiparkinsonian rats. *J Parkinsons Dis* 2014;4(3):349–360. [PubMed: 25061061]
20. Barnum CJ, Tansey MG. Modeling neuroinflammatory pathogenesis of Parkinson’s disease. *Prog Brain Res* 2010;184:113–132. [PubMed: 20887872]
21. Harms AS, Barnum CJ, Ruhn KA, et al. Delayed dominant-negative TNF gene therapy halts progressive loss of nigral dopaminergic neurons in a rat model of Parkinson’s disease. *Mol Ther* 2011;19(1):46–52. [PubMed: 20959812]
22. Sanchez-Guajardo V, Barnum CJ, Tansey MG, Romero-Ramos M. Neuroimmunological processes in Parkinson’s disease and their relation to alpha-synuclein: microglia as the referee between neuronal processes and peripheral immunity. *ASN Neuro* 2013;5(2):113–139. [PubMed: 23506036]
23. Cahoy JD, Emery B, Kaushal A, et al. A transcriptome database for astrocytes, neurons, and oligodendrocytes: a new resource for understanding brain development and function. *J Neurosci* 2008;28(1): 264–278. [PubMed: 18171944]
24. Reynolds RH, Botia J, Nalls MA, et al. Moving beyond neurons: the role of cell type-specific gene regulation in Parkinson’s disease heritability. *NPJ Parkinsons Dis* 2019;5:6. [PubMed: 31016231]
25. von Bartheld CS, Bahney J, Herculano-Houzel S. The search for true numbers of neurons and glial cells in the human brain: A review of 150 years of cell counting. *J Comp Neurol* 2016;524(18):3865–3895. [PubMed: 27187682]
26. Grabowski GA. Phenotype, diagnosis, and treatment of Gaucher’s disease. *Lancet* 2008;372(9645):1263–1271. [PubMed: 19094956]
27. Hruska KS, LaMarca ME, Scott CR, Sidransky E. Gaucher disease: mutation and polymorphism spectrum in the glucocerebrosidase gene (GBA). *Hum Mutat* 2008;29(5):567–583. [PubMed: 18338393]
28. Koprivica V, Stone DL, Park JK, et al. Analysis and classification of 304 mutant alleles in patients with type 1 and type 3 Gaucher disease. *Am J Hum Genet* 2000;66(6):1777–1786. [PubMed: 10796875]
29. Neumann J, Bras J, Deas E, et al. Glucocerebrosidase mutations in clinical and pathologically proven Parkinson’s disease. *Brain* 2009; 132(Pt 7):1783–1794. [PubMed: 19286695]
30. Sidransky E, Nalls MA, Aasly JO, et al. Multicenter analysis of glucocerebrosidase mutations in Parkinson’s disease. *N Engl J Med* 2009;361(17):1651–1661. [PubMed: 19846850]
31. Beavan M, McNeill A, Proukakis C, Hughes DA, Mehta A, Schapira AH. Evolution of prodromal clinical markers of Parkinson disease in a GBA mutation-positive cohort. *JAMA Neurol* 2015;72(2):201–208. [PubMed: 25506732]
32. Choi JH, Stubblefield B, Cookson MR, et al. Aggregation of alpha-synuclein in brain samples from subjects with glucocerebrosidase mutations. *Mol Genet Metab* 2011;104(1–2):185–188. [PubMed: 21742527]
33. Nalls MA, Duran R, Lopez G, et al. A multicenter study of glucocerebrosidase mutations in dementia with Lewy bodies. *JAMA Neurol* 2013;70(6):727–735. [PubMed: 23588557]
34. Alegre-Abarrategui J, Christian H, Lufino MM, et al. LRRK2 regulates autophagic activity and localizes to specific membrane microdomains in a novel human genomic reporter cellular model. *Hum Mol Genet* 2009;18(21):4022–4034. [PubMed: 19640926]
35. Eguchi T, Kuwahara T, Sakurai M, et al. LRRK2 and its substrate Rab GTPases are sequentially targeted onto stressed lysosomes and maintain their homeostasis. *Proc Natl Acad Sci U S A* 2018;115(39):E9115–E9124. [PubMed: 30209220]
36. Gardet A, Benita Y, Li C, et al. LRRK2 is involved in the IFN-gamma response and host response to pathogens. *J Immunol* 2010; 185(9):5577–5585. [PubMed: 20921534]
37. Hakimi M, Selvanantham T, Swinton E, et al. Parkinson’s disease-linked LRRK2 is expressed in circulating and tissue immune cells and upregulated following recognition of microbial structures. *J Neural Transm (Vienna)* 2011;118(5):795–808. [PubMed: 21552986]

38. Kozina E, Sadasivan S, Jiao Y, et al. Mutant LRRK2 mediates peripheral and central immune responses leading to neurodegeneration in vivo. *Brain* 2018;141(6):1753–1769. [PubMed: 29800472]
39. Schapansky J, Nardozi JD, Felizia F, LaVoie MJ. Membrane recruitment of endogenous LRRK2 precedes its potent regulation of autophagy. *Hum Mol Genet* 2014;23(16):4201–4214. [PubMed: 24682598]
40. Beilina A, Rudenko IN, Kaganovich A, et al. Unbiased screen for interactors of leucine-rich repeat kinase 2 supports a common pathway for sporadic and familial Parkinson disease. *Proc Natl Acad Sci U S A* 2014;111(7):2626–2631. [PubMed: 24510904]
41. Steger M, Tonelli F, Ito G, et al. Phosphoproteomics reveals that Parkinson’s disease kinase LRRK2 regulates a subset of Rab GTPases. *Elife* 2016;5.
42. Waschbusch D, Michels H, Strassheim S, et al. LRRK2 transport is regulated by its novel interacting partner Rab32. *PLoS One* 2014;9 (10):e111632. [PubMed: 25360523]
43. Reczek D, Schwake M, Schroder J, et al. LIMP-2 is a receptor for lysosomal mannose-6-phosphate-independent targeting of beta-glucocerebrosidase. *Cell* 2007;131(4):770–783. [PubMed: 18022370]
44. Tan YL, Genereux JC, Pankow S, Aerts JM, Yates JR 3rd, Kelly JW. ERdj3 is an endoplasmic reticulum degradation factor for mutant glucocerebrosidase variants linked to Gaucher’s disease. *Chem Biol* 2014;21(8):967–976. [PubMed: 25126989]
45. Yahalom G, Greenbaum L, Israeli-Korn S, et al. Carriers of both GBA and LRRK2 mutations, compared to carriers of either, in Parkinson’s disease: risk estimates and genotype-phenotype correlations. *Parkinsonism Relat Disord* 2019;62:179–184. [PubMed: 30573413]
46. Jana M, Jana A, Pal U, Pahan K. A simplified method for isolating highly purified neurons, oligodendrocytes, astrocytes, and microglia from the same human fetal brain tissue. *Neurochem Res* 2007;32(12):2015–2022. [PubMed: 17447141]
47. Suzuki K, Bose P, Leong-Quong RY, Fujita DJ, Riabowol K. REAP: a two minute cell fractionation method. *BMC Res Notes* 2010; 3:294. [PubMed: 21067583]
48. Motabar O, Goldin E, Leister W, et al. A high throughput glucocerebrosidase assay using the natural substrate glucosylceramide. *Anal Bioanal Chem* 2012;402(2):731–739. [PubMed: 22033823]
49. Theophilus B, Latham T, Grabowski GA, Smith FI. Gaucher disease: molecular heterogeneity and phenotype-genotype correlations. *Am J Hum Genet* 1989;45(2):212–225. [PubMed: 2502917]
50. Theophilus BD, Latham T, Grabowski GA, Smith FI. Comparison of RNase A, a chemical cleavage and GC-clamped denaturing gradient gel electrophoresis for the detection of mutations in exon 9 of the human acid beta-glucosidase gene. *Nucleic Acids Res* 1989;17(19):7707–7722. [PubMed: 2508065]
51. Ikuno M, Yamakado H, Akiyama H, et al. GBA haploinsufficiency accelerates alpha-synuclein pathology with altered lipid metabolism in a prodromal model of Parkinson’s disease. *Hum Mol Genet* 2019;28(11):1894–1904. [PubMed: 30689867]
52. Bae EJ, Yang NY, Lee C, et al. Loss of glucocerebrosidase 1 activity causes lysosomal dysfunction and alpha-synuclein aggregation. *Exp Mol Med* 2015;47:e188. [PubMed: 26427853]
53. Fernandes HJ, Hartfield EM, Christian HC, et al. ER stress and autophagic perturbations lead to elevated extracellular alpha-synuclein in GBA-N370S Parkinson’s iPSC-derived dopamine neurons. *Stem Cell Report* 2016;6(3):342–356.
54. Mazzulli JR, Xu YH, Sun Y, et al. Gaucher disease glucocerebrosidase and alpha-synuclein form a bidirectional pathogenic loop in synucleinopathies. *Cell* 2011;146(1):37–52. [PubMed: 21700325]
55. Schondorf DC, Aureli M, McAllister FE, et al. iPSC-derived neurons from GBA1-associated Parkinson’s disease patients show autophagic defects and impaired calcium homeostasis. *Nat Commun* 2014;5:4028. [PubMed: 24905578]
56. Fell MJ, Mirescu C, Basu K, et al. MLI-2, a potent, selective, and centrally active compound for exploring the therapeutic potential and safety of LRRK2 kinase inhibition. *J Pharmacol Exp Ther* 2015;355(3):397–409. [PubMed: 26407721]

57. Gloeckner CJ, Boldt K, von Zweyendorf F, et al. Phosphopeptide analysis reveals two discrete clusters of phosphorylation in the N-terminus and the Roc domain of the Parkinson-disease associated protein kinase LRRK2. *J Proteome Res* 2010;9(4):1738–1745. [PubMed: 20108944]
58. Lindstrom V, Gustafsson G, Sanders LH, et al. Extensive uptake of alpha-synuclein oligomers in astrocytes results in sustained intracellular deposits and mitochondrial damage. *Mol Cell Neurosci* 2017; 82:143–156. [PubMed: 28450268]
59. Loria F, Vargas JY, Bousset L, et al. Alpha-synuclein transfer between neurons and astrocytes indicates that astrocytes play a role in degradation rather than in spreading. *Acta Neuropathol* 2017; 134(5):789–808. [PubMed: 28725967]
60. Gegg ME, Burke D, Heales SJ, et al. Glucocerebrosidase deficiency in substantia nigra of parkinson disease brains. *Ann Neurol* 2012; 72(3):455–463. [PubMed: 23034917]
61. Murphy KE, Gysbers AM, Abbott SK, et al. Reduced glucocerebrosidase is associated with increased alpha-synuclein in sporadic Parkinson’s disease. *Brain* 2014;137(Pt 3):834–848. [PubMed: 24477431]
62. Tayebi N, Callahan M, Madike V, et al. Gaucher disease and parkinsonism: a phenotypic and genotypic characterization. *Mol Genet Metab* 2001;73(4):313–321. [PubMed: 11509013]
63. Tayebi N, Walker J, Stubblefield B, et al. Gaucher disease with parkinsonian manifestations: does glucocerebrosidase deficiency contribute to a vulnerability to parkinsonism? *Mol Genet Metab* 2003; 79(2):104–109. [PubMed: 12809640]
64. McNeill A, Duran R, Hughes DA, Mehta A, Schapira AH. A clinical and family history study of Parkinson’s disease in heterozygous glucocerebrosidase mutation carriers. *J Neurol Neurosurg Psychiatry* 2012;83(8):853–854. [PubMed: 22577228]
65. Kim CY, Alcalay RN. Genetic forms of Parkinson’s disease. *Semin Neurol* 2017;37(2):135–146. [PubMed: 28511254]
66. Beavan MS, Schapira AH. Glucocerebrosidase mutations and the pathogenesis of Parkinson disease. *Ann Med* 2013;45(8):511–521. [PubMed: 24219755]
67. Alcalay RN, Levy OA, Waters CC, et al. Glucocerebrosidase activity in Parkinson’s disease with and without GBA mutations. *Brain* 2015;138(Pt 9):2648–2658. [PubMed: 26117366]
68. Bultron G, Kacena K, Pearson D, et al. The risk of Parkinson’s disease in type 1 Gaucher disease. *J Inherit Metab Dis* 2010;33(2):167–173. [PubMed: 20177787]
69. Abramov AY, Canevari L, Duchen MR. Changes in intracellular calcium and glutathione in astrocytes as the primary mechanism of amyloid neurotoxicity. *J Neurosci* 2003;23(12):5088–5095. [PubMed: 12832532]
70. Brenner M, Johnson AB, Boespflug-Tanguy O, Rodriguez D, Goldman JE, Messing A. Mutations in GFAP, encoding glial fibrillary acidic protein, are associated with Alexander disease. *Nat Genet* 2001;27(1):117–120. [PubMed: 11138011]
71. Di Giorgio FP, Carrasco MA, Siao MC, Maniatis T, Eggan K. Non-cell autonomous effect of glia on motor neurons in an embryonic stem cell-based ALS model. *Nat Neurosci* 2007;10(5):608–614. [PubMed: 17435754]
72. Gu XL, Long CX, Sun L, Xie C, Lin X, Cai H. Astrocytic expression of Parkinson’s disease-related A53T alpha-synuclein causes neurodegeneration in mice. *Mol Brain* 2010;3:12. [PubMed: 20409326]
73. Nagele RG, D’Andrea MR, Lee H, Venkataraman V, Wang HY. Astrocytes accumulate A beta 42 and give rise to astrocytic amyloid plaques in Alzheimer disease brains. *Brain Res* 2003;971(2):197–209. [PubMed: 12706236]
74. di Domenico A, Carola G, Calatayud C, et al. Patient-specific iPSC-derived astrocytes contribute to non-cell-autonomous neurodegeneration in Parkinson’s disease. *Stem Cell Report* 2019;12(2):213–229.
75. Altshuler LL, Abulseoud OA, Foland-Ross L, et al. Amygdala astrocyte reduction in subjects with major depressive disorder but not bipolar disorder. *Bipolar Disord* 2010;12(5):541–549. [PubMed: 20712756]
76. Halliday GM, Stevens CH. Glia: initiators and progressors of pathology in Parkinson’s disease. *Mov Disord* 2011;26(1):6–17. [PubMed: 21322014]

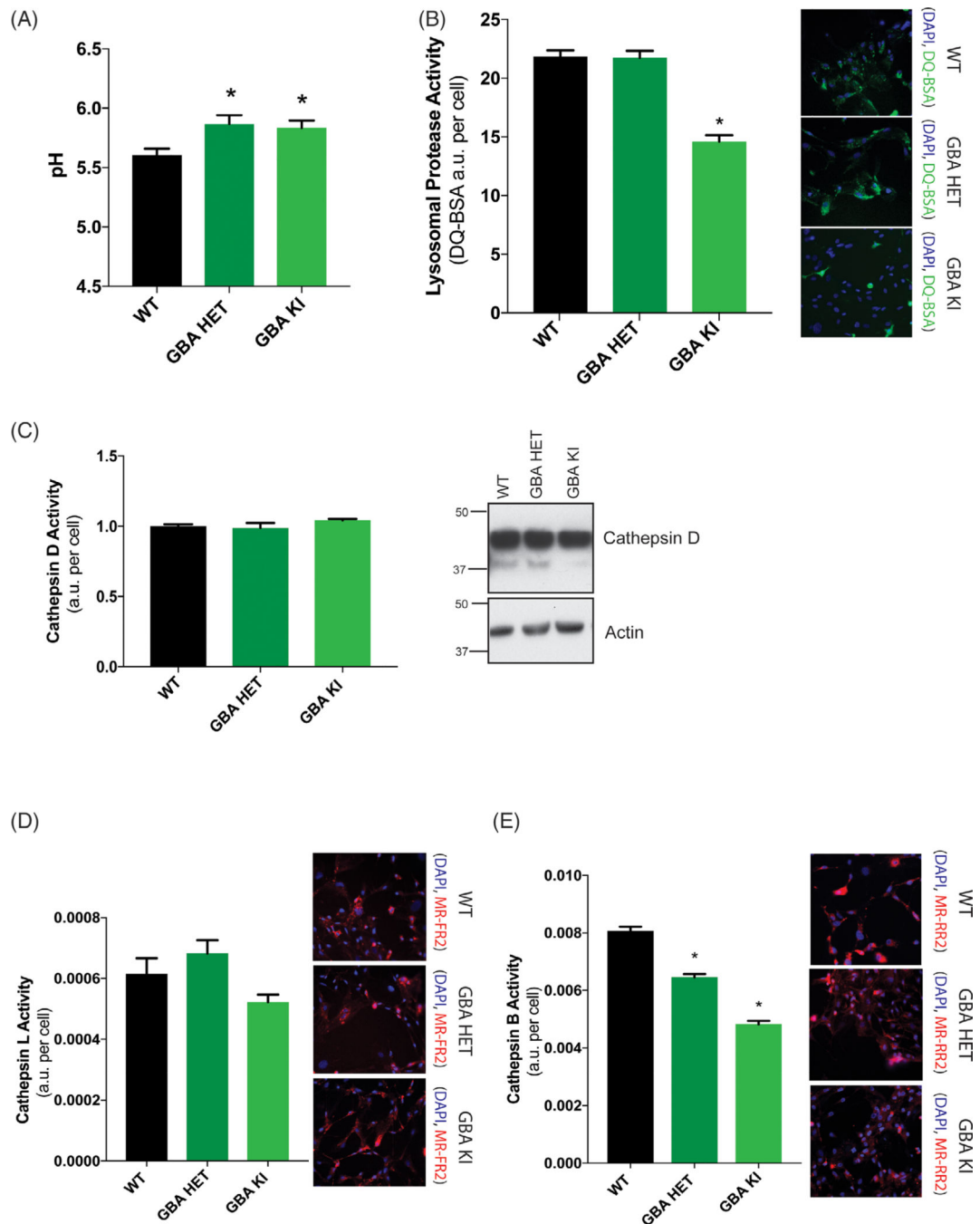
77. Heneka MT, Sastre M, Dumitrescu-Ozimek L, et al. Focal glial activation coincides with increased BACE1 activation and precedes amyloid plaque deposition in APP[V717I] transgenic mice. *J Neuroinflammation* 2005;2:22. [PubMed: 16212664]
78. Liddelow SA, Guttenplan KA, Clarke LE, et al. Neurotoxic reactive astrocytes are induced by activated microglia. *Nature* 2017; 541(7638):481–487. [PubMed: 28099414]
79. Orre M, Kamphuis W, Osborn LM, et al. Acute isolation and transcriptome characterization of cortical astrocytes and microglia from young and aged mice. *Neurobiol Aging* 2014;35(1):1–14. [PubMed: 23954174]
80. Pantazopoulos H, Woo TU, Lim MP, Lange N, Berretta S. Extracellular matrix-glia abnormalities in the amygdala and entorhinal cortex of subjects diagnosed with schizophrenia. *Arch Gen Psychiatry* 2010;67(2):155–166. [PubMed: 20124115]
81. Garcia-Sanz P, Orgaz L, Bueno-Gil G, et al. N370S-GBA1 mutation causes lysosomal cholesterol accumulation in Parkinson's disease. *Mov Disord* 2017;32(10):1409–1422. [PubMed: 28779532]
82. Lee HJ, Patel S, Lee SJ. Intravesicular localization and exocytosis of alpha-synuclein and its aggregates. *J Neurosci* 2005;25(25):6016–6024. [PubMed: 15976091]
83. Volpicelli-Daley LA, Luk KC, Lee VM. Addition of exogenous alpha-synuclein preformed fibrils to primary neuronal cultures to seed recruitment of endogenous alpha-synuclein to Lewy body and Lewy neurite-like aggregates. *Nat Protoc* 2014;9(9):2135–2146. [PubMed: 25122523]
84. Gustafsson G, Lindstrom V, Rostami J, et al. Alpha-synuclein oligomer-selective antibodies reduce intracellular accumulation and mitochondrial impairment in alpha-synuclein exposed astrocytes. *J Neuroinflammation* 2017;14(1):241. [PubMed: 29228971]
85. Song YJ, Halliday GM, Holton JL, et al. Degeneration in different parkinsonian syndromes relates to astrocyte type and astrocyte protein expression. *J Neuropathol Exp Neurol* 2009;68(10):1073–1083. [PubMed: 19918119]
86. Lee HJ, Suk JE, Patrick C, et al. Direct transfer of alpha-synuclein from neuron to astroglia causes inflammatory responses in synucleinopathies. *J Biol Chem* 2010;285(12):9262–9272. [PubMed: 20071342]
87. Schapansky J, Nardozi JD, LaVoie MJ. The complex relationships between microglia, alpha-synuclein, and LRRK2 in Parkinson's disease. *Neuroscience* 2015;302:74–88. [PubMed: 25284317]
88. Zhang Y, Chen K, Sloan SA, et al. An RNA-sequencing transcriptome and splicing database of glia, neurons, and vascular cells of the cerebral cortex. *J Neurosci* 2014;34(36):11929–11947. [PubMed: 25186741]
89. Ysselstein D, Nguyen M, Young TJ, et al. LRRK2 kinase activity regulates lysosomal glucocerebrosidase in neurons derived from Parkinson's disease patients. *Nat Commun* 2019;10(1):5570. [PubMed: 31804465]
90. Hirsch EC, Hunot S. Neuroinflammation in Parkinson's disease: a target for neuroprotection? *Lancet Neurol* 2009;8(4):382–397. [PubMed: 19296921]
91. Ouchi Y, Yoshikawa E, Sekine Y, et al. Microglial activation and dopamine terminal loss in early Parkinson's disease. *Ann Neurol* 2005;57(2):168–175. [PubMed: 15668962]
92. Miklossy J, Doudet DD, Schwab C, Yu S, McGeer EG, McGeer PL. Role of ICAM-1 in persisting inflammation in Parkinson disease and MPTP monkeys. *Exp Neurol* 2006;197(2):275–283. [PubMed: 16336966]
93. Sathe K, Maetzler W, Lang JD, et al. S100B is increased in Parkinson's disease and ablation protects against MPTP-induced toxicity through the RAGE and TNF-alpha pathway. *Brain* 2012; 135(Pt 11):3336–3347. [PubMed: 23169921]
94. Barcia C, Ros CM, Annese V, et al. IFN-gamma signaling, with the synergistic contribution of TNF-alpha, mediates cell specific microglial and astroglial activation in experimental models of Parkinson's disease. *Cell Death Dis* 2012;3:e379. [PubMed: 22914327]
95. Jaumotte JD, Castro SL, Smeyne RJ, Zigmond MJ. Isolated housing decreases the immune response in sera and brain following exposure to a bacterial toxin in older rats. Paper presented at: Annual Meeting of the Society for Neuroscience; 2016; San Diego, CA. 11 12–16.

**FIG. 1.**

*GBA1 D409V* knockin mutation causes morphologic defects in the lysosomes of primary murine astrocytes. **(A)** Flow cytometry analysis (left panel) of primary mouse astrocyte cultures stained with GFAP detected in Q3 and ~2% microglial contamination detected in Q4. These cultures, analyzed by immunofluorescence assay (right panel) detecting astrocytes stained with GFAP (red), microglia stained with Cd11B (green) and neurons stained with NeuN (yellow) reveal similar levels of microglial contamination. Nucleus is stained with DAPI (blue). **(B)** Immunologic responsiveness of WT astrocytes tested by LPS

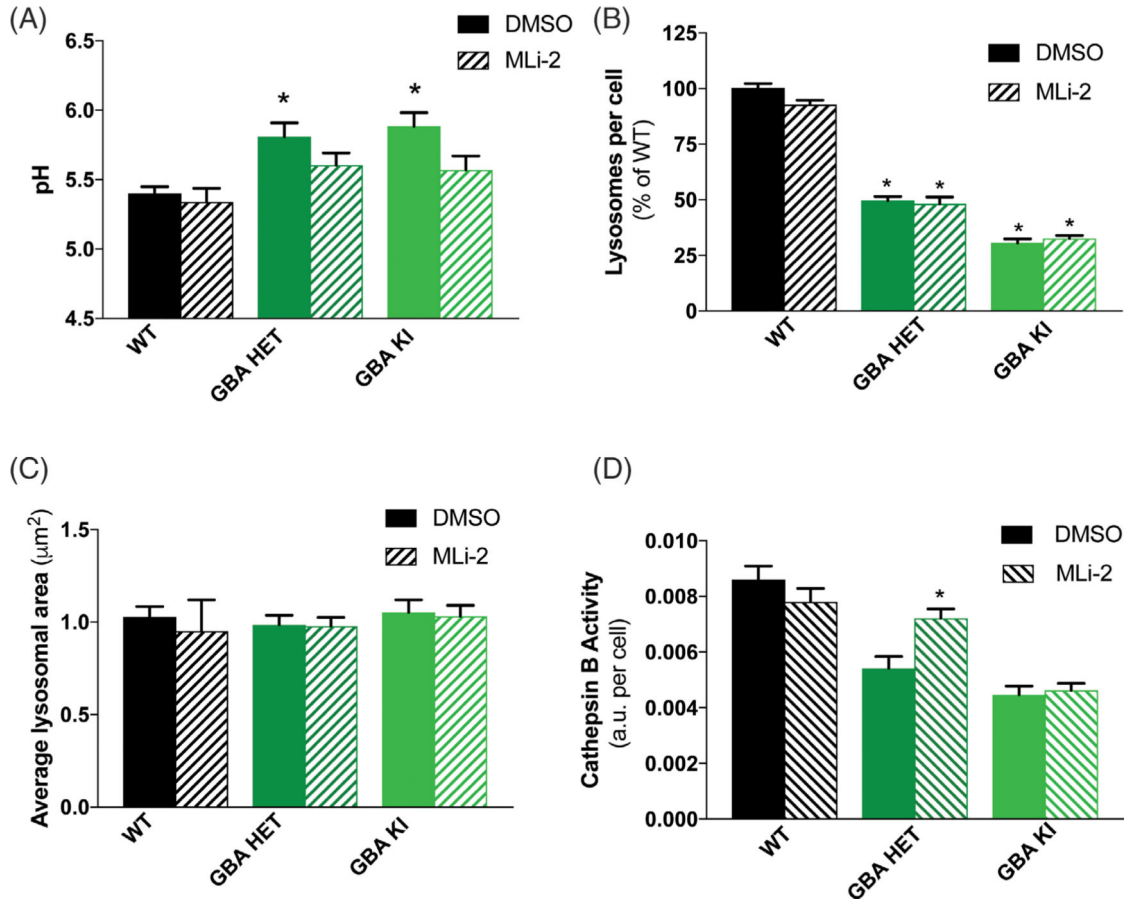


induction (100 ng/mL or 50 EU/mL; 6 and 24 hours) display a classic TLR4-dependent upregulation of IL6, IL1 $\beta$ , TNF, and iNOS mRNA (N = 3). (C) GCCase activity assay using GCCase-specific fluorogenic substrate show 47% activity in heterozygous (GBA HET) and 8% activity in homozygous (GBA KI) knockin astrocytes. CBE treatment almost completely inhibits GCCase activity, confirming specificity of the assay (N = 3). High-content image analysis, as detected by LysoTracker staining normalized to number of cells, show (D) a significant decrease in the lysosomal numbers in heterozygous (GBA HET) and homozygous (GBA KI) knockin astrocytes and (E) unchanged average lysosomal area in these cells. Yellow fluorescence from LysoTracker staining is observed in representative microscopy images. All lysosomal analyses were collated from 3 independent experiments with 20 wells per genotype per experiment (N = 3, F = 49,  $P < 0.0001$ ). (F) Protein expression of lysosomal genes, LAMP1, GCCase, and nTFEB was not affected by *GBA1* mutation, as detected by Western blot. Actin was used as a loading control (G). The immunofluorescence of LAMP1 (red) and LAMP2 (green) shows reduced colocalization of LAMP1 at lysosomes detected by LAMP2 in heterozygous (Spearman's rank correlation of 0.49; GBA HET) and homozygous (Spearman's rank correlation of 0.45; GBA KI) knockin astrocytes when compared with WT (Spearman's rank correlation of 0.56). Nuclei are detected by DAPI (blue) stain. \* $P < 0.05$ , analysis of variance followed by Tukey's post hoc test. Cd11B, integrin alpha M subunit.

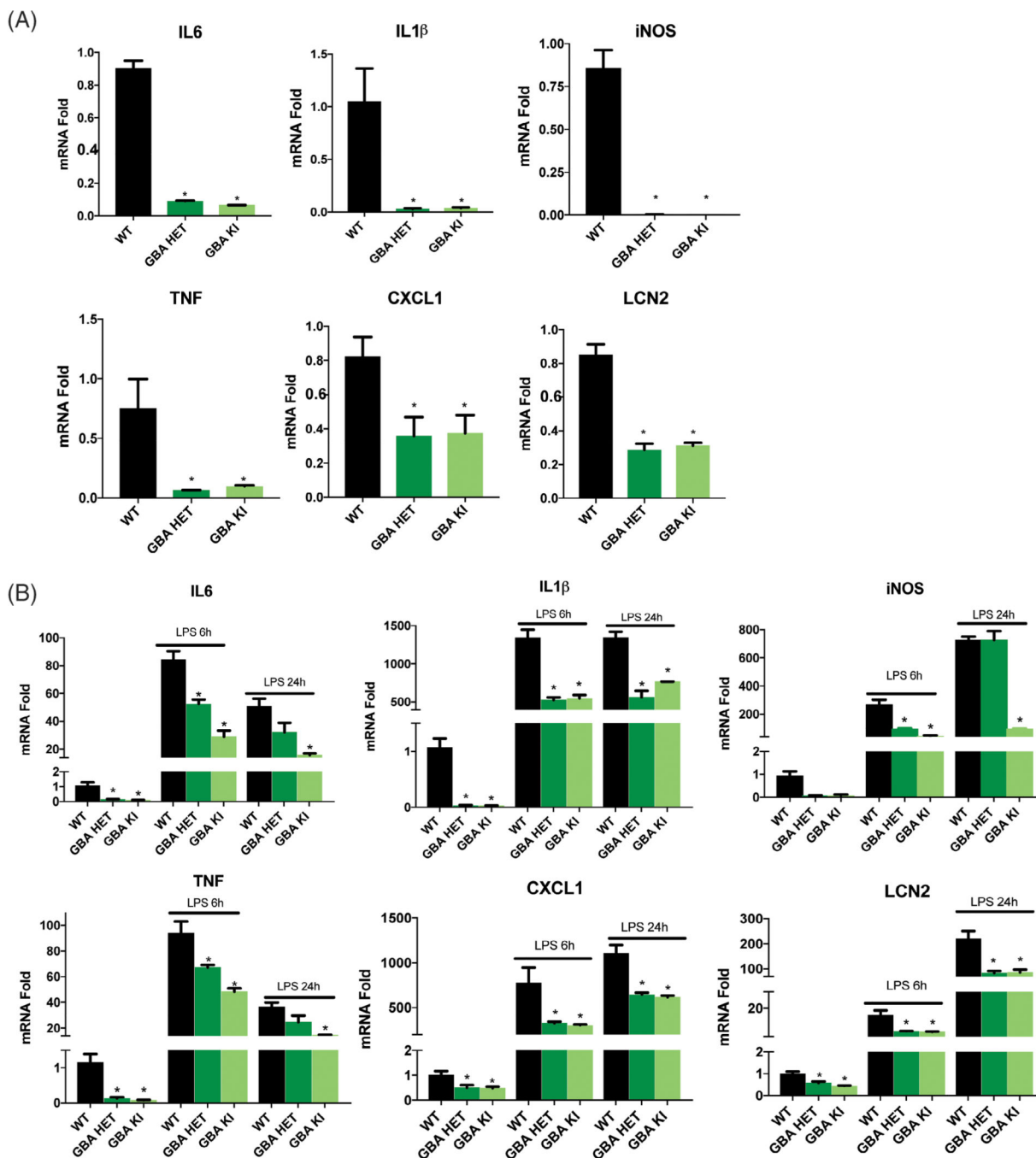
**FIG. 2.**

*GBA1 D409V* knockin mutation reduces lysosomal protease activity. **(A)** Determination of lysosomal pH using LysoSensor displays increased alkalinization to pH 6 in heterozygous (GBA HET) and homozygous (GBA KI) knockin astrocytes. Data are collated from 3 independent experiments with 20 wells per genotype ( $N = 3$ ,  $F = 5.017$ ,  $P = 0.0089$ ). **(B)** General lysosomal protease activity, as detected by DQ-BSA cleavage (green), shows a significant reduction in homozygous (GBA HET), but not heterozygous (GBA KI), knockin astrocytes. Green fluorescence as a result of cleavage of DQ-BSA is observed in

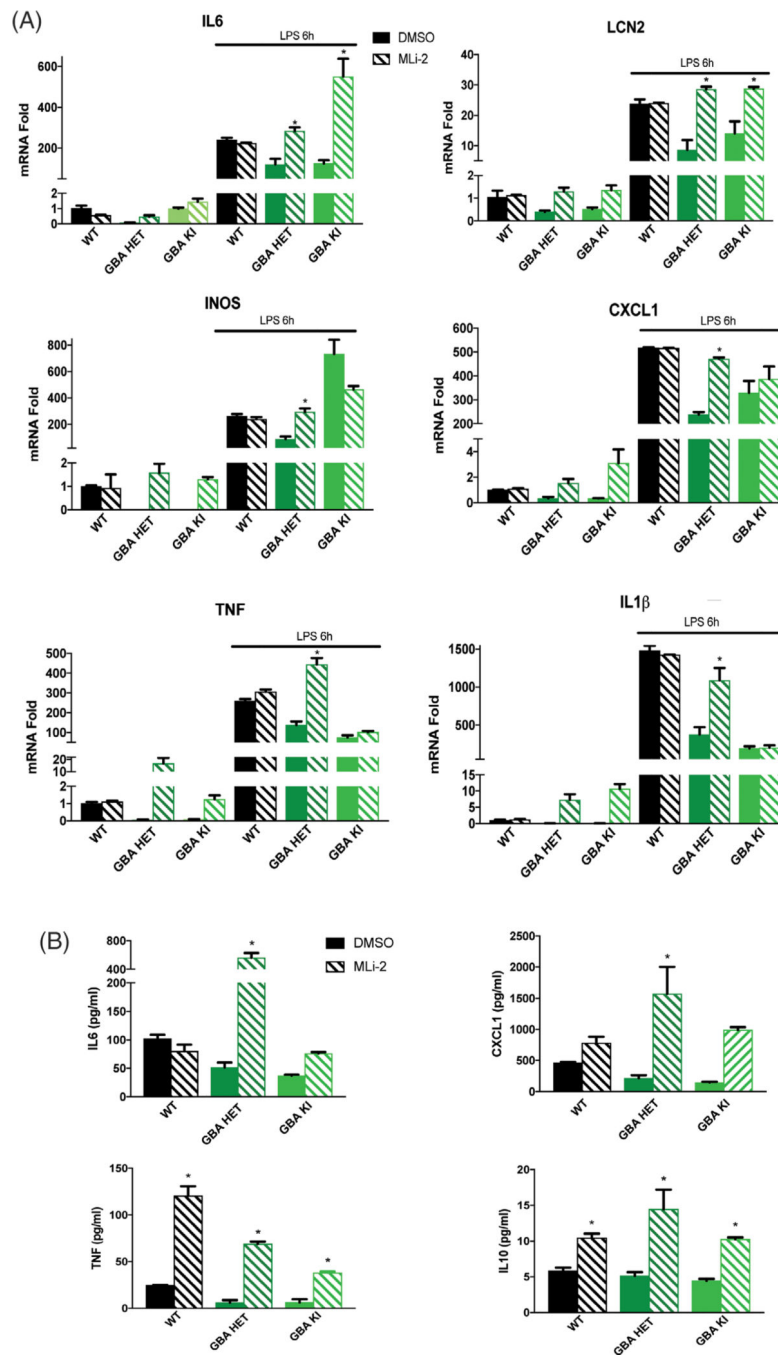
representative microscopy images ( $N = 3$ ,  $F = 55.41$ ,  $P < 0.0001$ ). (C) Cathepsin D activity, as detected by cathepsin D activity assay and Western blot of cathepsin D protein band and (D) cathepsin L activity, as detected by cleavage of Magic-Red substrate (red), exhibit no change as a result of a *GBA1* mutation ( $N = 3$ ,  $F = 3,783$ ,  $P = 0.0309$ ). (E) Cathepsin B activity, as detected by cleavage of Magic-Red substrate (red), show a significant dose-dependent reduction in heterozygous (GBA HET) and homozygous (GBA KI) knockin astrocytes. Red fluorescence from cathepsin B/L-specific substrate cleavage is observed in representative microscopy images ( $N = 3$ ,  $F = 161.3$ ,  $P < 0.0001$ ). In all fluorogenic plate-based activity assays, the nuclei were detected by Hoechst 33258 (blue) for normalization of the fluorescent signal. Data were collated from 3 independent experiments with 5 to 10 wells per genotype per experiment ( $N = 3$ ). \* $P < 0.05$ , analysis of variance followed by Tukey's post hoc test.

**FIG. 3.**

LRRK2 kinase inhibition rescues lysosomal defects caused by the *GBA1 D409V* mutation. (A) 3 days treatment with the LRRK2 kinase inhibitor, MLI-2 (15 nM), normalizes *GBA1*-mutant lysosomes to pH ~5.5 while not affecting WT lysosomal pH ( $N = 3$ ,  $F = 8.731$ ,  $P < 0.0001$ ). (B) Lysosomal number ( $N = 3$ ,  $F = 220.6$ ,  $P < 0.0001$ ) and (C) average lysosomal area in WT and *GBA1*-mutant astrocytes remain unaffected by MLI-2 treatment. (D) 7 days treatment with MLI-2 (15 nM) rescues cathepsin B activity, as detected by enzyme-specific Magic-Red dye cleavage in heterozygous (GBA HET), but not homozygous (GBA KI), knockin astrocytes ( $N = 3$ ,  $F = 31.53$ ,  $P < 0.0001$ ). All lysosomal analyses were collated from 3 independent experiments with 10 wells per genotype per experiment ( $N = 3$ ). Two-way analysis of variance followed by Tukey's post hoc test.

**FIG. 4.**

*GBA1 D490V* knockin astrocytes show dysregulated inflammatory responses. Quantitative polymerase chain reaction of (A) basal and (B) LPS-induced (100 ng/mL or 50 EU/mL, 6 and 24 hours) proinflammatory cytokines IL6, IL1 $\beta$ , TNF, and Interleukin 12 and chemokines iNOS, CXCL1, LCN2 show significant reductions of mRNA levels in *GBA1*-mutant astrocytes when compared with WT astrocytes. Data are normalized to actin expression and collated from 3 independent experiments including 3 biological replicates per experiment (N = 3). \* $P < 0.05$ , analysis of variance followed by Tukey's post hoc test.

**FIG. 5.**

MLi-2 normalizes the deficits in inflammatory response caused by *GBA1 D409V* knockin mutation. (A) Quantitative polymerase chain reaction of MLI-2 treated (15 nM, 3 days) and LPS-induced (100 ng/mL or 50 EU/mL, 6 hours) proinflammatory cytokines IL6, IL1 $\beta$ , TNF, and IL12p70 and chemokines iNOS, CXCL1, and LCN2 in *GBA1*-mutant astrocytes display normalization of mRNA expression to WT levels when compared with the DMSO-treated control. Data are normalized to actin expression and collated from 3 independent experiments including 3 biological replicates per experiment (N = 3). \* $P < 0.05$ , analysis of

variance followed by Tukey's post hoc test. **(B)** Meso Scale Discovery (Rockville, MD) immunoassay of MLI-2 treated (15 nM, 3 days) basal levels of proinflammatory cytokines IL6, IL10, and TNF and chemokine CXCL1 secreted in the conditioned media show robust normalization beyond WT levels (n = 3). \* $P < 0.05$ , analysis of variance followed by Tukey's post hoc test.

Author Manuscript

Author Manuscript

Author Manuscript

Author Manuscript